MASSACHUSETTS INSTITUTE OF TECHNOLOGY

LINCOLN LABORATORY

A SIMPLE METHOD FOR DESIGNING AN ELLIPTICAL POLARIZER IN SQUARE WAVEGUIDE

Alvin H. Kessler

William J. Getsinger

28 May 1963

The work reported in this document was performed at Lincoln Laboratory, a center for research operated by Massachusetts Institute of Technology, with the Joint support of the U.S. Army, Navy and Air Force under Air Force Contract AF 19(628)-500.

LEXINGTON MASSACHUSETTS

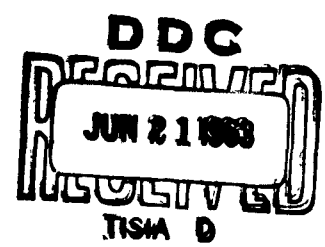

ABSTRACT

This paper shows a procedure that was used to find the differential phase shift between the two orthogonal $TE_{1,0}$ modes that synthesize an elliptically polarized wave in a modified square waveguide by deriving simple algebraic expressions for the cut-off wavelengths of the two modes. The results achieved indicate that the approximations caused less than 1.5 percent error over the applicable range of interest.

A SIMPLE METHOD FOR DESIGNING AN ELLIPTICAL POLARIZER IN SQUARE WAVEGUIDE

It is generally known that a square waveguide can propagate an elliptically polarized wave and that this wave can be analyzed as two spatially orthogonal $TE_{1,0}$ modes.[1]

A common problem is to transform a single $TE_{1,0}$ mode into an elliptically polarized mode. A device that does this is called an elliptical polarizer. One possible approach for constructing an elliptical polarizer is a square waveguide in which two diagonally opposite corners have been cut off.

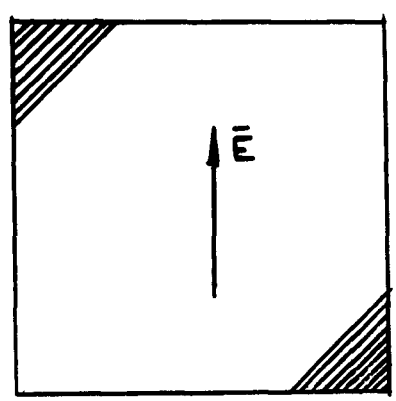

Figure 1

Electric Field Vector Incident on a Modified Square Waveguide

A wave in the $TE_{1,0}$ mode incident upon the polarizer as shown in Fig. 1 can be considered to be made up of two components, one having its electric field, $E_{//}$, parallel to the cut corners (as in Fig. 2a), and the other having its electric field, $E_{\perp}$, perpendicular to the cut corners (Fig. 2d).

The phase velocity of each orientation or mode is different because the boundary conditions are geometrically different. Therefore, a difference in phase will result as the two modes travel through the polarizer.

As an example, a circular polarizer can be made by adjusting the height and length of the corner ridges to give a 90° difference in phase between the two components over the length of the polarized section. To accomplish this, the cut-off wavelengths of the two modes must be known in the region of the modified corners.

The cut-off wavelengths can be determined by using a calculus of variations technique.[2] This paper will demonstrate a less formidable approach that gives very simple algebraic formulas, usable with negligible error for most design problems.

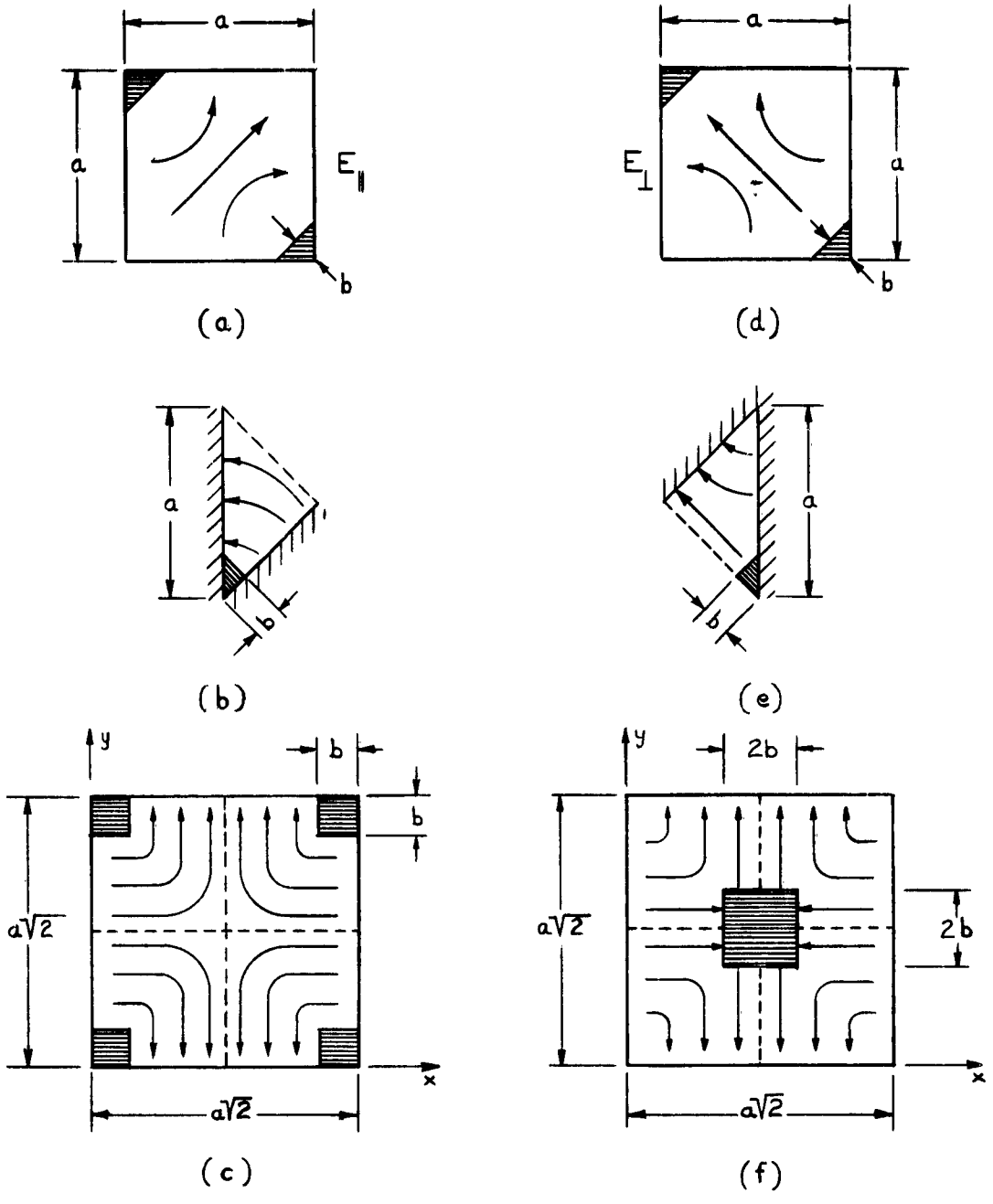

Fig. 2. The Electric Fields of:

(a) The $E_{\parallel}$ mode of the polarizer
(b) The triangular section of (a) and (c) chosen for solution
(c) The $TE_{1,1}$ mode perturbed by four square-corner bars
(d) The $E_{\perp}$ mode of the polarizer
(e) The triangular section of (d) and (f) chosen for solution
(f) The $TE_{1,1}$ mode perturbed by a square axial bar

Consider the solution for the $E_{//}$ mode indicated in Fig. 2a. The fields of this mode will be undisturbed by an electric wall passed corner to corner and perpendicular to the electric field lines. Similarly, a magnetic wall can be placed through the other two corners parallel to the electric field. It is then necessary to consider only that triangular portion of the original square waveguide bounded by the electric wall, the magnetic wall, and one of the initial walls.

One of these triangular sections is shown in Fig. 2b. Because its fields and geometry are identical with those in the waveguide of Fig. 2a, it will therefore have the same cut-off wavelength.

The larger square waveguide of Fig. 2c, shown propagating the $TE_{1,1}$ mode, has the same cut-off wavelength as does the small triangular waveguide of Fig. 2b. This can be seen by observing that magnetic walls can be passed center to center through opposite walls of the waveguide in Fig. 2c, and that electric walls may be placed corner to corner without disturbing the fields of the $TE_{1,1}$ mode. When that has been done, the fields within a triangular section formed by a magnetic wall, an electric wall, and part of the original waveguide wall, will be identical with those of the small triangular section of Fig. 2b (which was itself derived from the $E_{//}$ mode of Fig. 2a). Therefore, the cut-off wavelength of the $E_{//}$ mode in Fig. 2a is the same as that of the $TE_{1,1}$ mode of Fig. 2c. Also, the two cut corners shown in Fig. 2a correspond to the four square bars pictured in Fig. 2c. The effect of these bars upon the cut-off wavelength will be determined by perturbation theory.

Perturbation theory deals with the change in the resonant frequency of a cavity that has had a small volumetric change. It may be said that the cut-off frequency is of interest here and not the resonant frequency. However, if the waveguide is operated at its cut-off frequency, it is possible to make use of

the fact that the waveguide is in resonance, and therefore its cut-off frequency and resonant frequency become synonymous.

Reasoning similar to that used above holds for the $E_{\perp}$ mode of Fig. 2d, but now the cut corners correspond to a single bar placed axially in the larger waveguide carrying the $TE_{1,1}$ mode.

Consider now a unit length of the waveguide of Fig. 2c, supporting the $TE_{1,1}$ mode at its cut-off frequency, to be a resonator. Then, the change in resonant frequency, Δf, arising from the perturbation caused by the four bars, can be obtained by rewriting Slater's perturbation theorem, [3] as

$$\frac{\Delta f}{f_o} = \frac{\Delta U_E - \Delta U_H}{2U_o} \tag{1}$$

The unperturbed resonant frequency is f_o; ΔU_E and ΔU_H are the peak electric and magnetic energies over the perturbation, respectively, and U_o is the total stored-energy in the resonant structure. In the region of the perturbing rods, $\Delta U_H \gg \Delta H_E$.

$$\Delta U_H = \frac{1}{2} \mu |H_z|^2 \Delta V, \tag{2}$$

where ΔV is the perturbing volume. With the proper choice of origin,

$$H_z = B \cos\left(\frac{\pi x}{a\sqrt{2}}\right) \cos\left(\frac{\pi y}{a\sqrt{2}}\right), \tag{3}$$

where the quantity B is an arbitrary constant. If ΔV is small, then H_z will be fairly constant in that region and ΔU_H can be approximated by evaluating H_z at the point,

$$x = y = \frac{b}{2}, \tag{4}$$

$$\Delta U_H \cong -2 \mu b^2 B^2 \left[1 - \left(\frac{\pi b}{2a}\right)^2\right]. \tag{5}$$

The total energy stored at resonance can be found from the peak magnetic field,

$$U_o = \frac{1}{2}\mu \int_0^{a\sqrt{2}} \int_0^{a\sqrt{2}} |H_z|^2 \, dxdy = \frac{1}{4}\mu B^2 a^2 . \qquad (6)$$

Note that the energies are evaluated per unit length in the axial direction. This is possible because at cut-off the fields in the axial direction remain constant. Using Equations (1) through (6),

$$\frac{\Delta f}{f_o} \cong 4\left(\frac{b}{a}\right)^2 \left[1 - \left(\frac{\pi b}{2a}\right)^2\right] . \qquad (7)$$

Also,

$$\frac{\Delta f}{f_o} = -\frac{\Delta\lambda}{\lambda_o} , \qquad (8)$$

where $\Delta\lambda$ is defined as,

$$\Delta\lambda = (\lambda_c)_{E_{//}} - \lambda_o . \qquad (9)$$

The quantity $(\lambda_c)_{E_{//}}$ is the cut-off wavelength of the perturbed $TE_{1,1}$ mode and therefore also of the $E_{//}$ mode; λ_o is the cut-off wavelength of the unperturbed $TE_{1,1}$ mode, and in a square waveguide $a\sqrt{2}$ on a side,

$$\lambda_o = 2a. \qquad (10)$$

Using Equations (7) through (10), the cut-off wavelength of the $E_{//}$ mode of Fig. 2a becomes,

$$\frac{(\lambda_c)_{E_{//}}}{2a} \cong 1 - 4\left(\frac{b}{a}\right)^2 + \pi^2\left(\frac{b}{a}\right)^4 . \qquad (11)$$

A graph of Equation (11) appears in Fig. 3.

The solution for the cut-off wavelength of the $E_{\perp}$ mode of Fig. 2d is similar to that for the $E_{/\!/}$ mode. However, it must be remembered that now the perturbing volume is one axial bar, as shown in Fig. 2f, instead of the four corner bars used in the $E_{/\!/}$ calculations. Also, $\Delta U_E \gg \Delta U_H$; and,

$$\Delta U_E = -\frac{1}{2} \epsilon \left[E_x^2 + E_y^2 \right] \Delta V, \tag{12}$$

where

$$E_x = j\frac{\eta\sqrt{2}}{2} B \cos\left(\frac{\pi x}{a\sqrt{2}}\right) \sin\left(\frac{\pi y}{a\sqrt{2}}\right) . \tag{13}$$

The quantity ΔU_E can be approximated by evaluating E_x and E_y at the point

$$x = y = \frac{a}{\sqrt{2}} - \frac{b}{2} . \tag{14}$$

At this point,

$$E_x = -E_y . \tag{15}$$

Using Equations (12) through (15),

$$\Delta U_E \cong -\frac{1}{4} \mu B^2 b^2 \left(\frac{\pi b}{a}\right)^2 ; \tag{16}$$

and, from Equations (1), (6), and (16),

$$\frac{\Delta f}{f_o} \cong -\frac{\pi^2}{2} \left(\frac{b}{a}\right)^4 . \tag{17}$$

Substitution into Equations (7) through (9) leads then to the cut-off wavelength of the $E_{\perp}$ mode,

$$\frac{(\lambda_c)_{E_{\perp}}}{2a} = 1 + \frac{\pi^2}{2} \left(\frac{b}{a}\right)^4 . \tag{18}$$

A plot of Equation (18) appears in Fig. 3.

Equations (11) and (18) agree very well with results obtained by applying calculus of variations to the problem. The results from the analysis used here have less than 1.5 percent error for $(\lambda_c)_{E_{//}}$ in the region $0 < \frac{b}{a} < 0.36$, and less than 0.75 percent for $(\lambda_c)_{E_{\perp}}$ over the same region. The approximation for $E_{\perp}$ is fairly good in the range beyond (b/a) = 0.36, but the approximation for $E_{//}$ falls off rapidly after that, having 6.6 percent error at (b/a) = 0.4. However, a larger value of (b/a) would be undesirable for most applications, because such a large change in waveguide shape would give impedance matching problems and tend to generate and propagate higher order modes.

Since this device will function as a polarizer, the difference in phase between the two orthogonal modes, $E_{//}$ and $E_{\perp}$, over a length, ℓ, of a square waveguide with triangular corner sections is of importance, and will be called the differential phase shift, θ_D.

$$\theta_D = \theta_{//} - \theta_{\perp} = 2\pi\ell \left[\frac{1}{\lambda_{g_{//}}} - \frac{1}{\lambda_{g_{\perp}}} \right], \qquad (19)$$

where the phase shifts, $\theta_{//}$ and $\theta_{\perp}$, and the guide wavelengths, $\lambda_{g_{//}}$ and $\lambda_{g_{\perp}}$, refer respectively to the $E_{//}$ and $E_{\perp}$ modes. A plot of Eq. (19), the differential phase shift, as applied to the flat ridge section appears in Fig. 4. In Figs. 4 and 5 the quantity α (voltage attenuation in nepers per meter) having a non-zero value simply shows that one of the modes has reached a cut-off condition.

The construction of this device in practice necessitates the addition of tapers to each end of the triangular ridge sections to provide an acceptable impedance match. It therefore becomes important to know how much phase shift these tapers will add in addition to that of the flat corner sections. This can be determined experimentally by choosing a reasonable length for a set of tapers

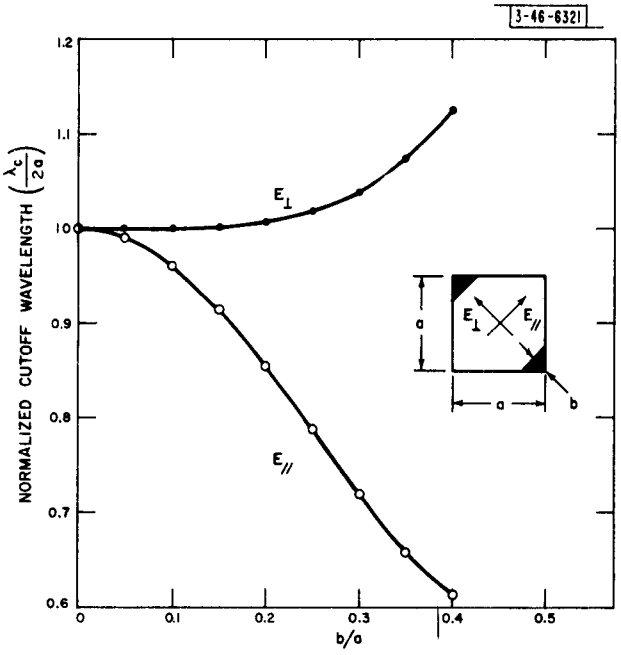

Fig. 3. Cutoff wavelengths of the $E_{//}$ and $E_\perp$ modes vs. ridge height.

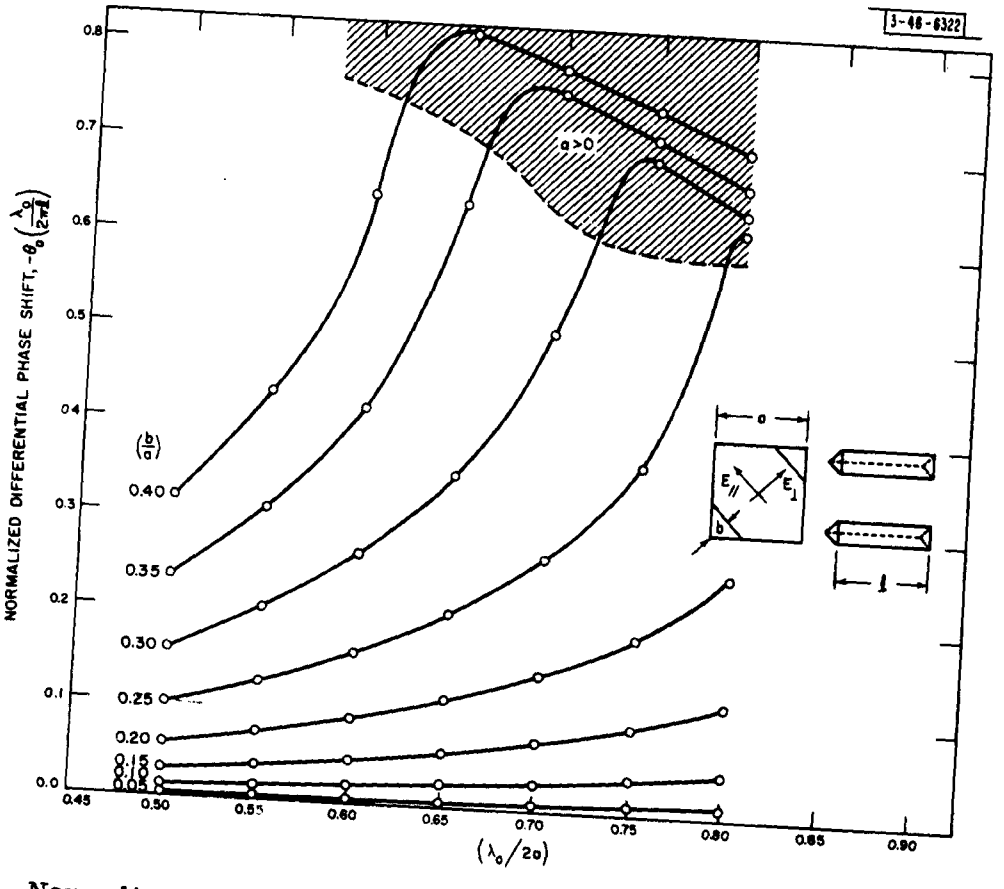

Fig. 4. Normalized differential phase shift for a set of flat ridge sections.

and building a model so that the total differential phase shift of the device can be measured. The differential phase shift of the tapers can then be found by subtracting the phase shift of the middle untapered section, as computed from Eq. (19), from the total measured differential phase shift.

It is then possible to construct a polarizer with any desired amount of phase shift using the tapers just measured and a new middle untapered section designed from Eq. (19) to provide the remainder of the required phase shift.

The exact phase shift of the tapered sections can be expressed mathematically by considering the following analysis for linear tapers.

In Eqs. (11) and (18), if the quantity, b, is replaced by the quantity (bx/L), where x is now the length parameter that is variable, and L is the length of the tapers, the cut-off wavelengths of the two modes, $E_{/\!/}$ and $E_{\perp}$, as a function of the position along the tapers, x, become

$$(\lambda_c)_{E_{/\!/}} \cong 2a\left[1 - 4\left(\frac{bx}{aL}\right)^2 + \pi^2\left(\frac{bx}{aL}\right)^4\right], \tag{20}$$

and

$$(\lambda_c)_{E_{\perp}} \cong 2a\left[1 + \frac{\pi^2}{2}\left(\frac{bx}{aL}\right)^4\right].$$

The total phase shift for each orientation is then

$$\theta_{/\!/} \cong \frac{2\pi}{\lambda_o}\int_o^L \sqrt{1 - \left\{\frac{\lambda_o}{2a\left[1 - 4\left(\frac{bx}{aL}\right)^2 + \pi^2\left(\frac{bx}{aL}\right)^4\right]}\right\}^2}\, dx, \tag{22}$$

and

$$\theta_{\perp} \cong \frac{2\pi}{\lambda_o}\int_o^L \sqrt{1 - \left\{\frac{\lambda_o}{2a\left[1 + \frac{\pi^2}{2}\left(\frac{bx}{aL}\right)^4\right]}\right\}^2}\, dx. \tag{23}$$

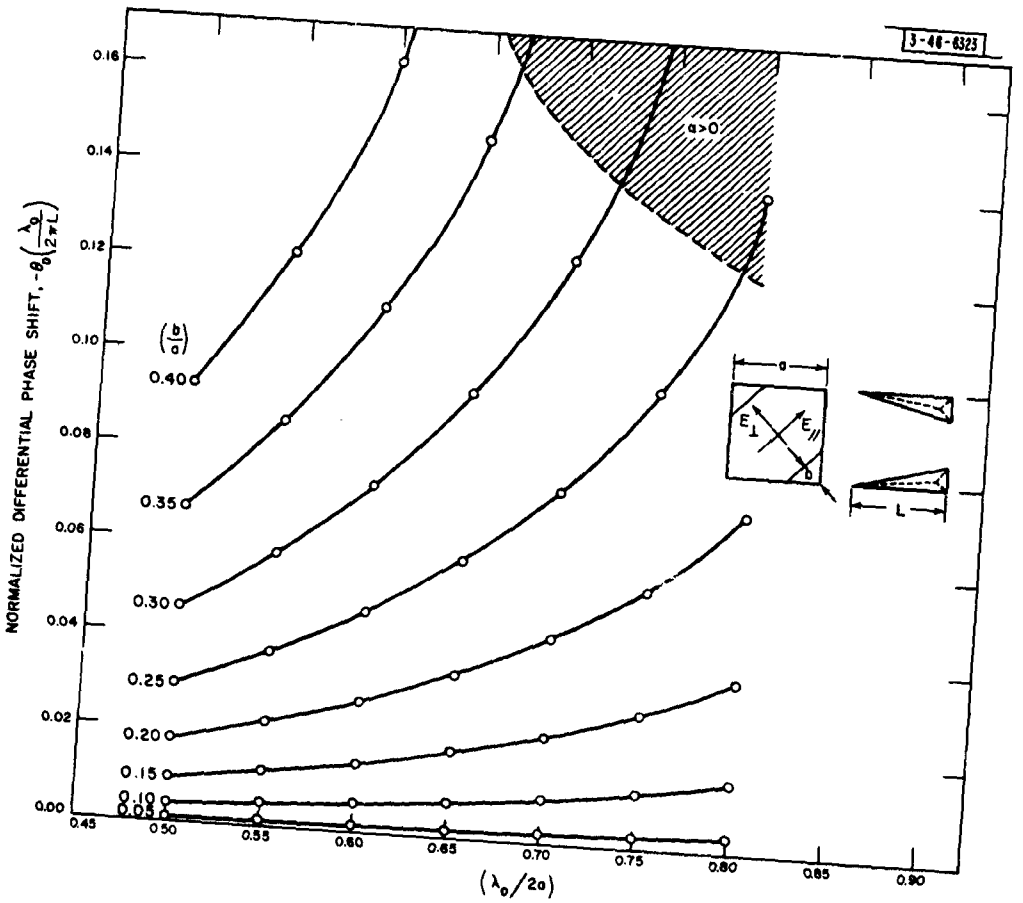

Fig. 5. Normalized differential phase shift for a set of linear tapers

The integration of Equations (22) and (23) was performed numerically by computer techniques. The results obtained for the total differential phase shift, θ_D, for a set of linear tapers of length, L, are plotted in Fig. 5.

Lastly, it must be noted that Figs. 4 and 5 do not take into account a small additional phase shift resulting from the change in waveguide impedance through the phase shifter. Therefore, using Figs. 4 and 5, one can completely design a phase shifter that will yield a result very close but not exactly equal to the predicted values.

ACKNOWLEDGMENT

The authors would like to acknowledge the work of Mr. Craig Work, of Group 81, who handled all of the computer programming.

AHK:mfm

REFERENCES

(1) G. L. Ragan, Microwave Transmission Circuits, Radiation Laboratory Series, Volume 9, 369-373 (McGraw-Hill Book Company, Inc., 1948). This article refers to circular waveguide, but is readily applicable to square waveguide also.

(2) A forthcoming Lincoln Laboratory technical report by R. N. Assaly of Group 61.

(3) J. C. Slater, Microwave Electronics, 81-83 (D. Van Nostrand Company, Inc., Princeton, New Jersey, 1950).

DISTRIBUTION LIST

C. W. Jones
J. Freedman (Division 4)
W. Andrews
C. Blake
W. Both
A. Browne
K. Keeping
E. Maxwell
E. McCurley
S. Miller
C. Muehe
F. Dominick
W. Getsinger (12)
A. Kessler (24)
L. Bowles
B. LaPage (Group 61)
R. Assaly (Group 61)